

## Supplementary Information

Dynamic organic crystal as exceptionally efficient artificial natural  
light-harvesting actuator

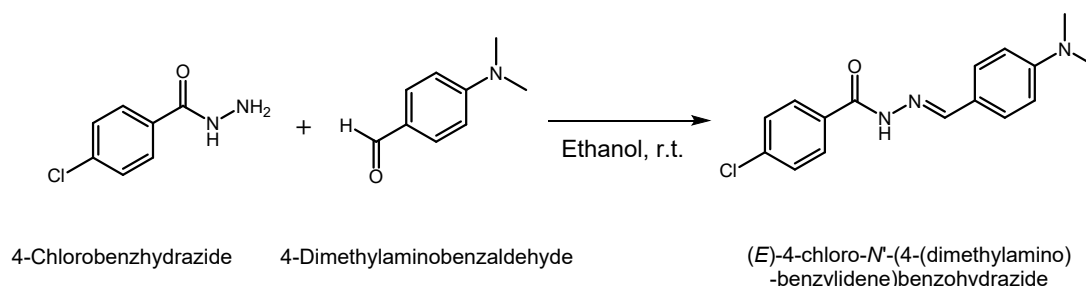
Zhu et al.

## Experimental section

### Materials

4-Chlorobenzhydrazide (98%), 4-Dimethylaminobenzaldehyde (99%) were purchased from Bide Pharmatech CO., Ltd. Ethyl alcohol was purchased from Rionlon Bohua (Tianjin) Pharmaceutical & Chemical Co., Ltd. N-Hexane was purchased from Anonji Chemical Technology Co., Ltd. Dichloromethane was purchased from Meryer (Shanghai) Chemical Technology Co., Ltd. All of the reagents were used without further purification.

### Synthesis Method



**Scheme S1.** Synthesis of the (E)-4-chloro-N'-(4-(dimethylamino)benzylidene)benzohydrazide (CDBB).

As shown in Scheme S1, 4-Chlorobenzhydrazide (0.34g, 0.002mol) and 4-Dimethylaminobenzaldehyde (0.30g, 0.002mol) were dissolved in ethanol (20 mL) separately, which were subsequently mixed together. The solution was subjected to magnetic agitation for 14h, and the product would be precipitated. The suspension solution was filtered, and the filter cake was washed by ethanol. Finally, the product with a yield of 68% with no further purification was obtained.

### Crystallization of Form I and Form II

Form I and Form II were derived by applying solvent diffusion method. Firstly, CDBB was dissolved in dichloromethane in a test tube, and then appropriate n-hexane was added slowly to the tube to form two phase, which would let n-hexane diffuse to the solution very slowly. After four days of diffusion, plate-like Form I grew at the bottom of the test tube, and needle-like Form II was obtained at the two-phase interface.

### General Characterization

#### Molecular structures

$^1\text{H}$  NMR spectra were recorded on a Bruker 400 MHz spectrometer to confirm the molecular structure of the synthesized compounds. Spectra were collected in Dimethyl sulfoxide- $d_6$  (DMSO- $d_6$ ) and chloroform- $d$  ( $\text{CDCl}_3$ ) solution.

### **Single crystal X-ray diffraction**

A suitable single crystal was set on an XtaLAB Synergy-Custom system with HyPix detector (Rigaku). The data was collected at -173.15 °C and -160.15 °C, while controlling the temperature with a Cryostream 800 cooler (Oxford Cryosystems). Olex2 was used to solve the structure by intrinsic phasing methods (SHELXT).

### **Powder X-ray diffraction**

Powder X-ray diffraction (PXRD) was performed on a Rigaku D/MAX 2500 with the parameters of Cu Ka radiation are 1.5405 Å, 2-35° and 10°/min.

### **Thermal properties**

Thermal Gravimetric Analyze (TGA) and Differential Scanning Calorimetry (DSC) were performed with a TGA/DSC system (Mettler Toledo, Co., Switzerland) with heating rates of 10 °C·min<sup>-1</sup>.

### **Fluorescence spectroscopy**

Fluorescence spectra were tested by a photoluminescence spectrometer (Edinburgh Instruments, FLS1000, UK).

### **Hot-stage measurements**

Hot-stage microscopic measurements were carried out by a Linkam system including a temperature-controlled stage LNP94/2 mounted on a microscope CX40P. The heating rate is 10 °C·min<sup>-1</sup>.

### **Microscopy**

All the videos were recorded by a digital high-speed microscope (Keyence, VHX-5000, Japan) and a high-speed camera Nikon Z7, at a speed of 120 frames per second.

### **UV induced photomechanical effects of CDBB**

The light source for photoirradiation was a Height LED HTLD-4 UV-LED light source (UV-light, 365 nm).

### **Fourier Transform Infrared Spectrometer**

Fourier Transform Infrared (FTIR) Spectrometer of the polymorphs were collected using a Bruker Alpha FTIR with 4 cm<sup>-1</sup> resolution and 16 scans per spectrum at 4000–400 cm<sup>-1</sup> range. UV-Vis spectra were collected on PerkinElmer LAMBDA750.

## **Theoretical calculations**

### **Conformation and energy barriers for isomerization**

The restricted optimization of the molecular structure was firstly carried out by Gaussian 09 based on single crystal data at B3LYP/6-311G(d,p) level. Then, potential energy surface scanning was carried out at the B3LYP/6-311G(d,p) level, with the dihedral angle around the C=N double bond as the variable at the step of 5° to obtain the potential energy curves. The first guess structure of *cis*-molecule and transition state was obtained according to the potential energy surface curves. On the basis of the first guess structure, the transition state search and *cis*-molecular structure optimization were further performed under B3LYP/6-311G(d,p) level, respectively. After obtaining the transition states, the calculations of single point energy for the *cis*-, *trans*- and transition state structures were carried out under M06-2X/DEF2-TZVP level. Finally, the energy barriers for different processes were obtained according to the single point energy.

### **Intermolecular interaction analysis**

The interaction energy frameworks for Form I and Form II were calculated by using Crystal Explorer 17.

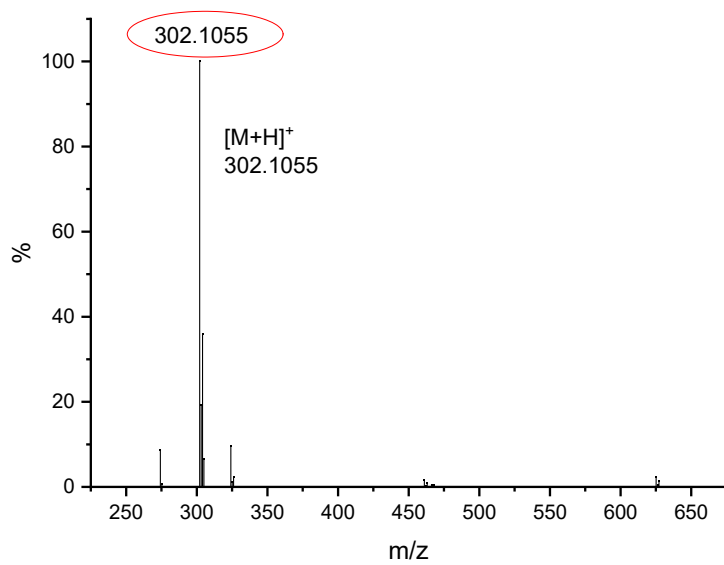


**Figure S1.** HRMS (ESI) spectrum of CDBB.

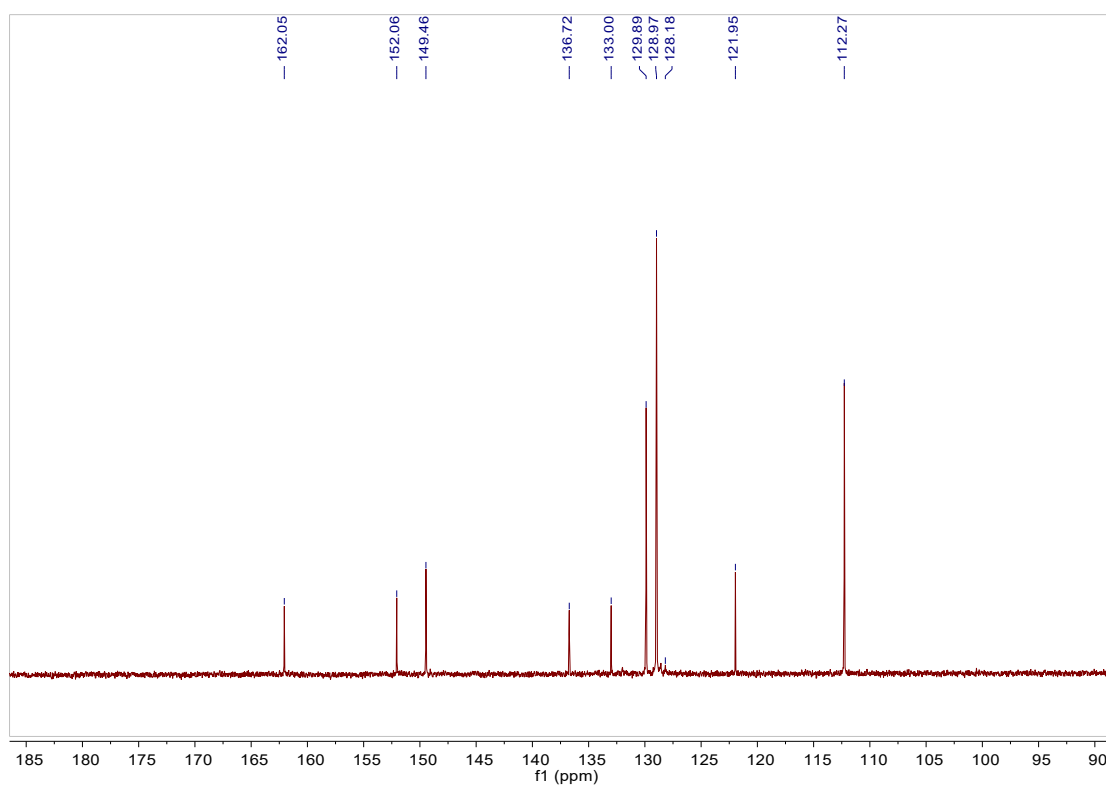


**Figure S2.** <sup>13</sup>C NMR spectrum of CDBB in DMSO-d<sub>6</sub>.

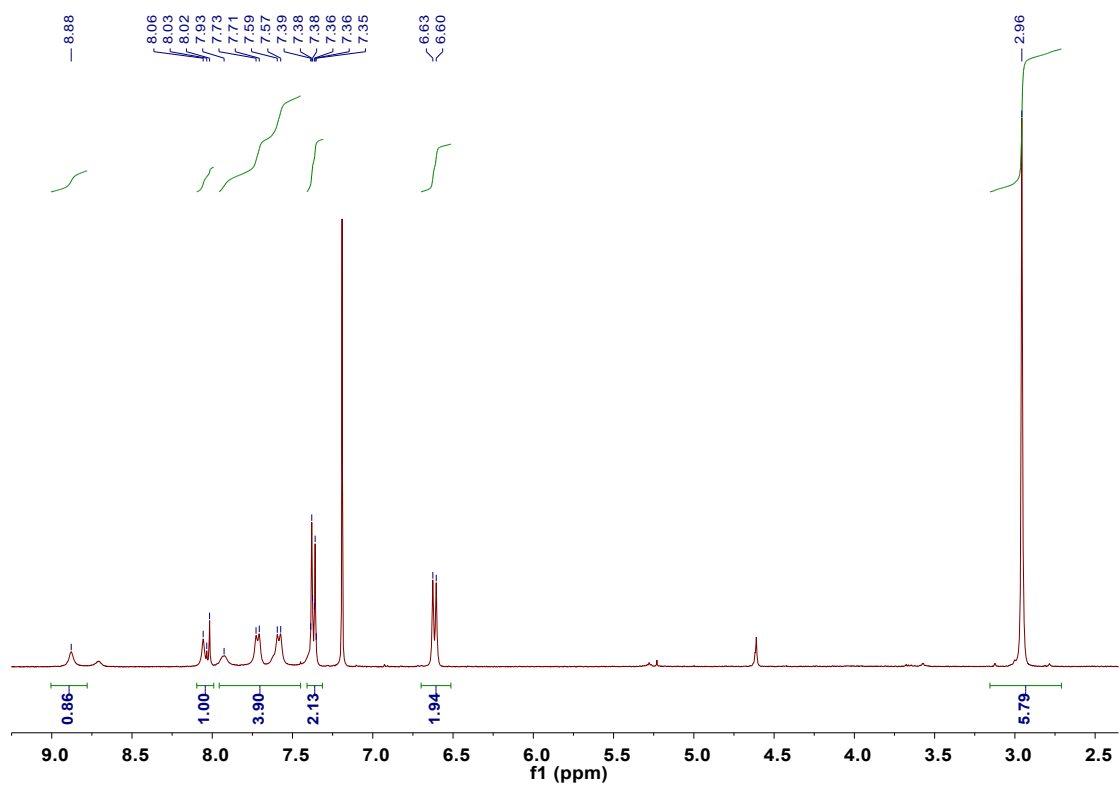


**Figure S3.** <sup>1</sup>H NMR (400 MHz, Chloroform-*d*) δ 8.88 (s, 1H), 8.04 (d,  $J = 16.1$  Hz, 1H), 7.95 – 7.45 (m, 4H), 7.41 – 7.32 (m, 2H), 6.62 (d,  $J = 8.5$  Hz, 2H), 2.96 (s, 6H).

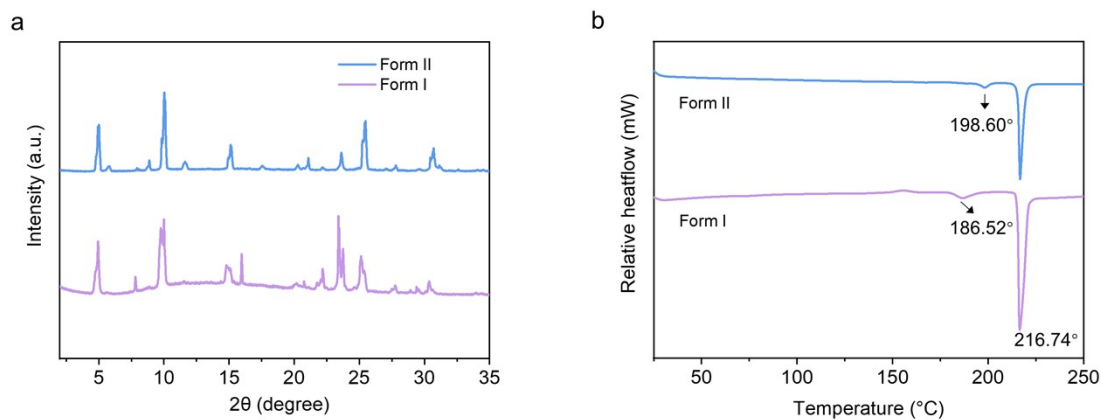


**Figure S4.** (a) Powder X-ray diffraction (PXRD) patterns and (b) Differential Scanning Calorimetry (DSC) curves of Form I and Form II.

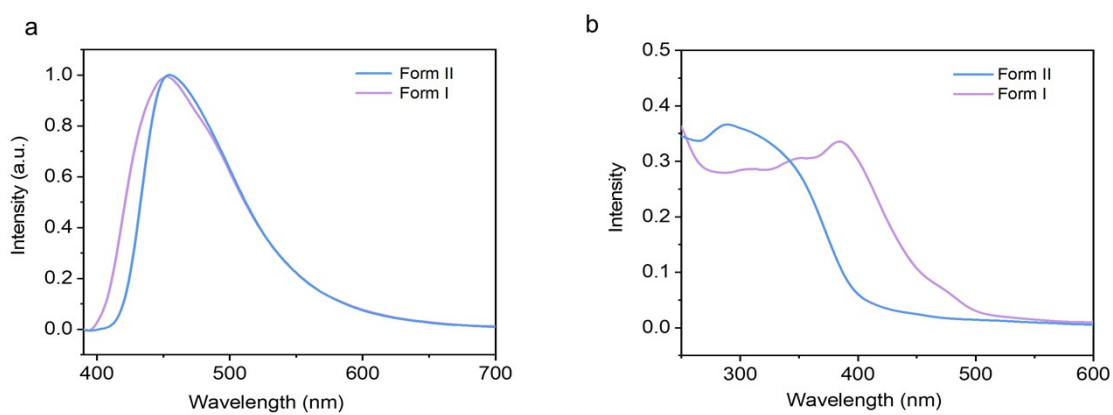


**Figure S5.** (a) Fluorescence spectra and (b) UV-Vis absorption spectra of Form I and Form II.

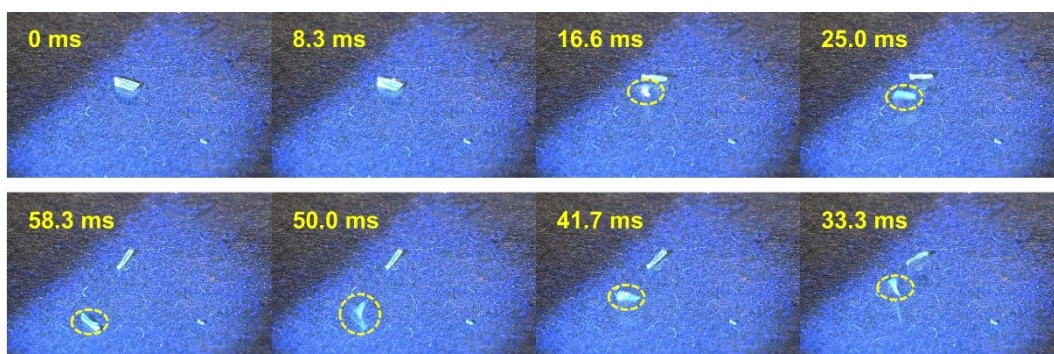


**Figure S6.** Photosalient effects of Form I captured by high-speed camera upon UV irradiation (365nm).

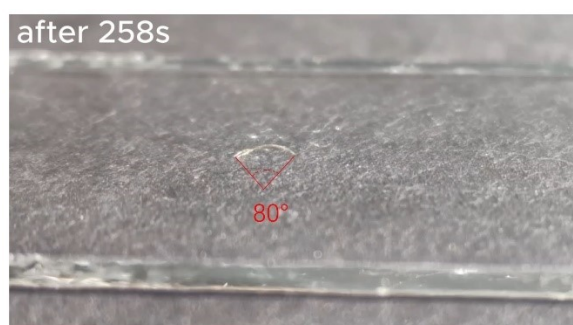


**Figure S7.** Photoinduced bending of Form I before jumping under sunlight.

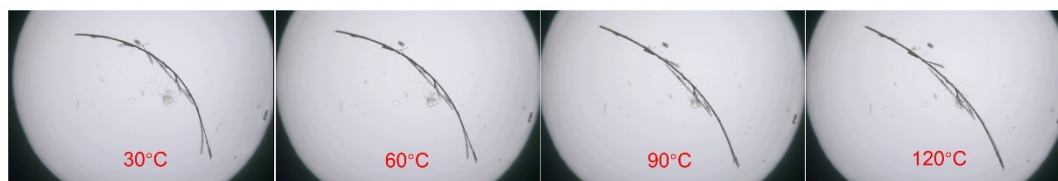


**Figure S8.** The unbending process of Form II upon heating.



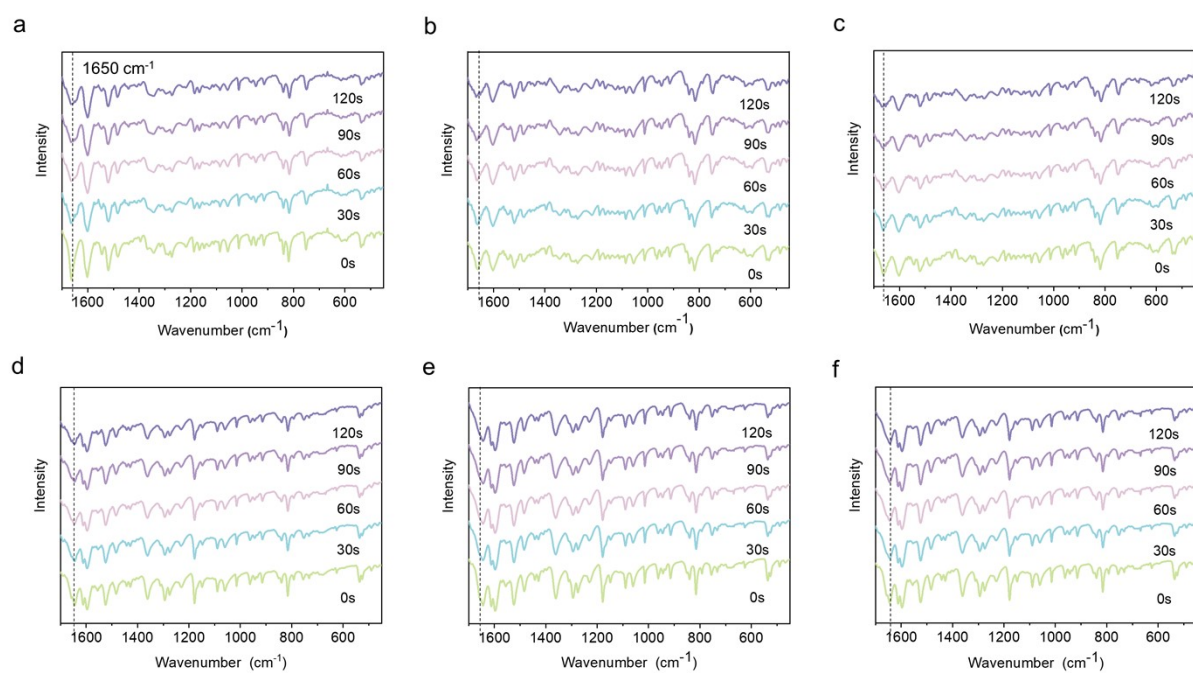


**Figure S9.** Time-dependent Fourier transform infrared (FTIR) spectra upon sunlight, 425nm and 365nm LEDs irradiation of Form I (a-c) and Form II (d-f).

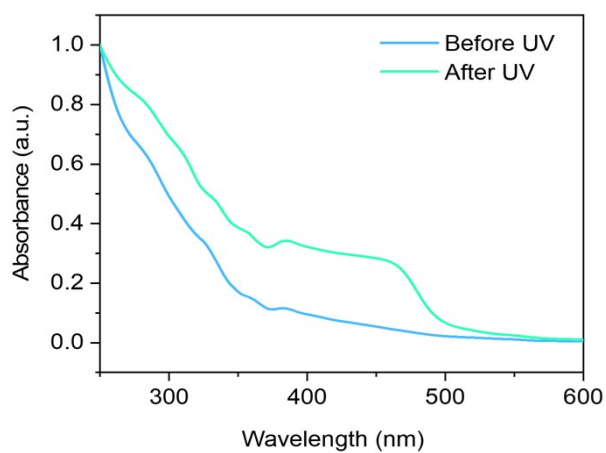


**Figure S10.** UV-vis spectra of Form II upon irradiation.

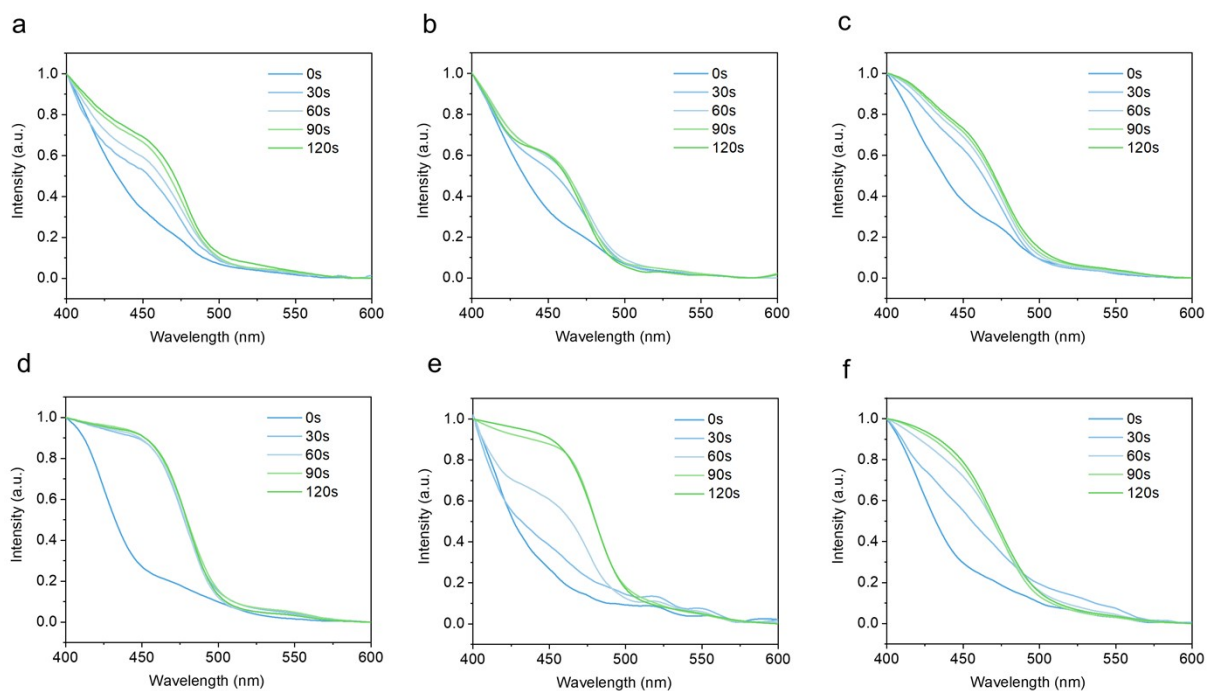


**Figure S11.** Time-dependent UV-Vis absorption upon sunlight, 425nm and 365nm LEDs irradiation of Form I (a-c) and Form II (d-f).

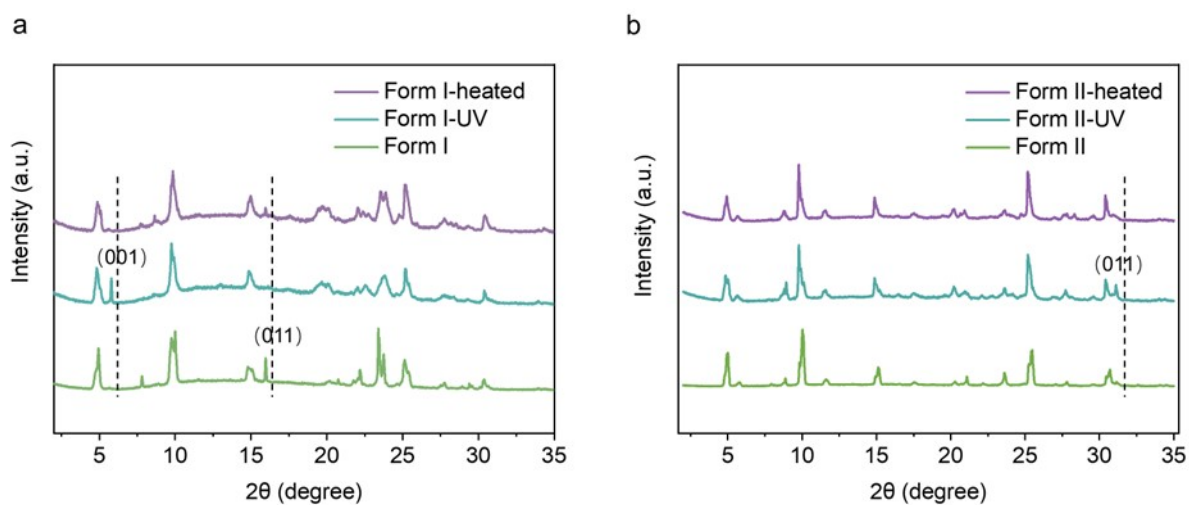


**Figure S12.** PXRD patterns of Form I (a) and Form II (b) upon UV irradiation and heating.

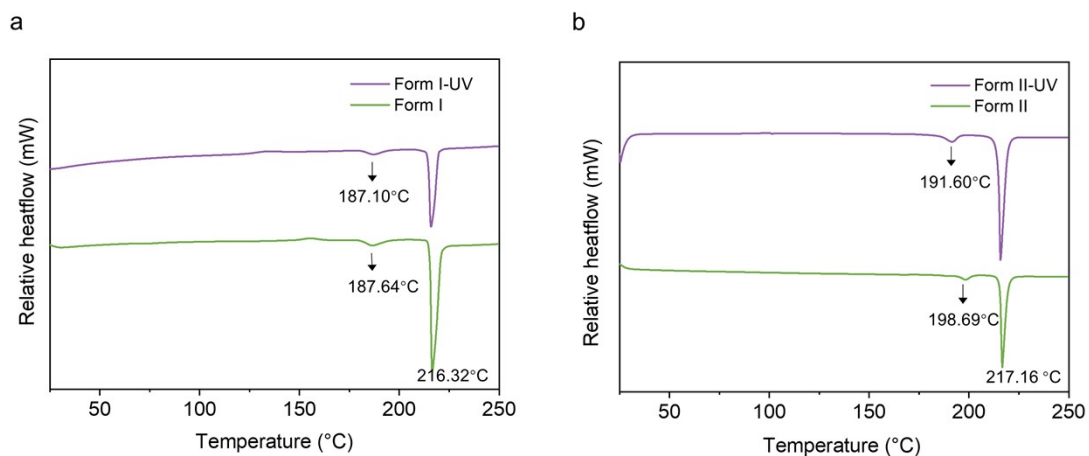


**Figure S13.** DSC curves of Form I (a) and Form II (b) before and after UV irradiation.

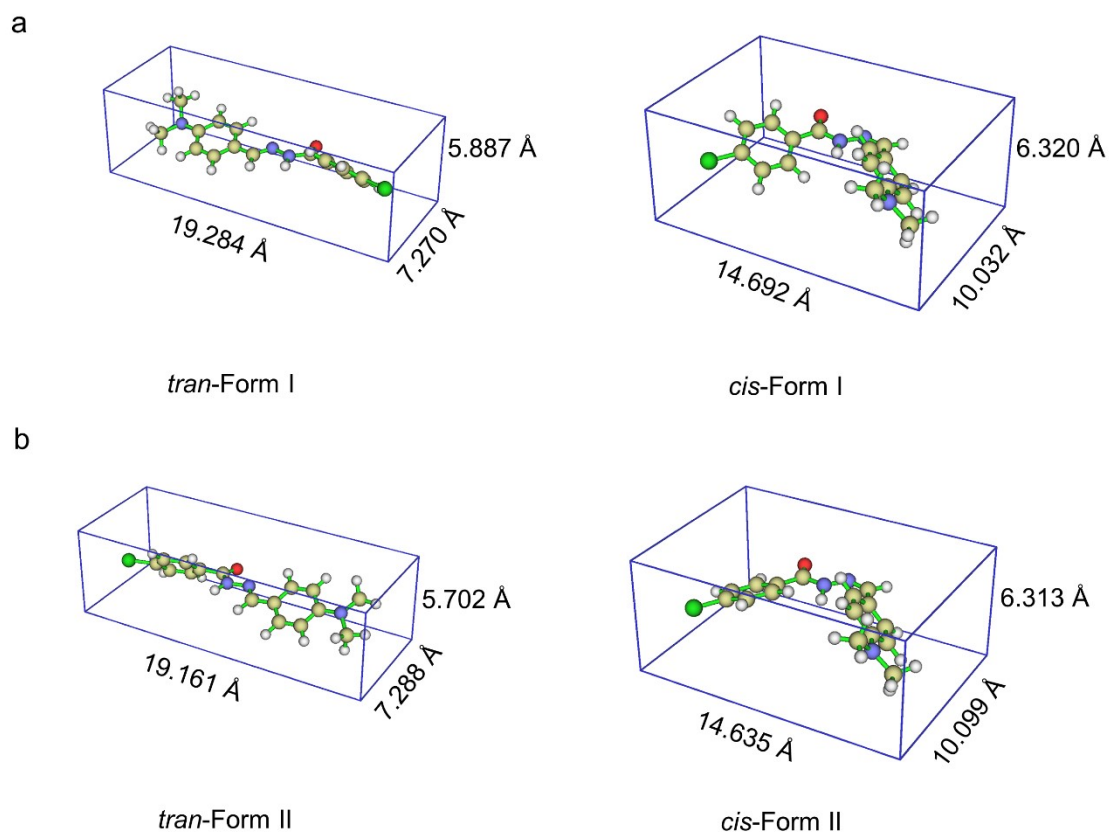


**Figure S14.** Molecular volume change after isomerization of Form I (a) and Form II (b).

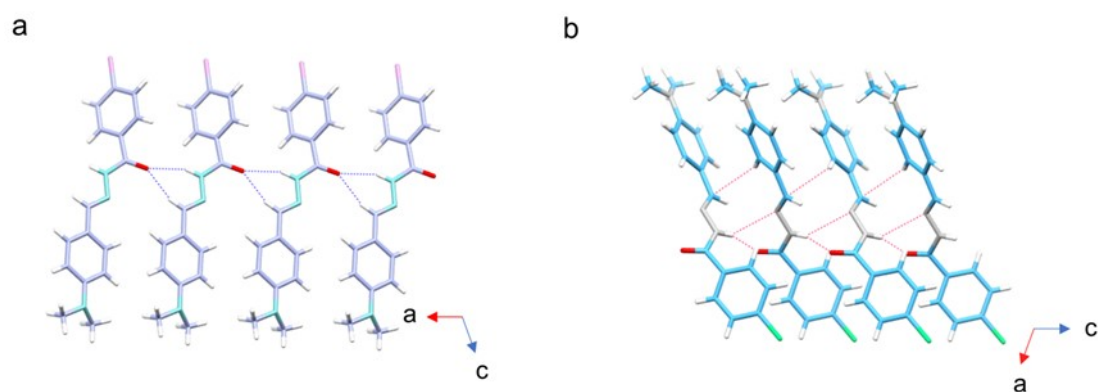


**Figure S15.** Intermolecular interactions of Form I (a) and Form II (b).

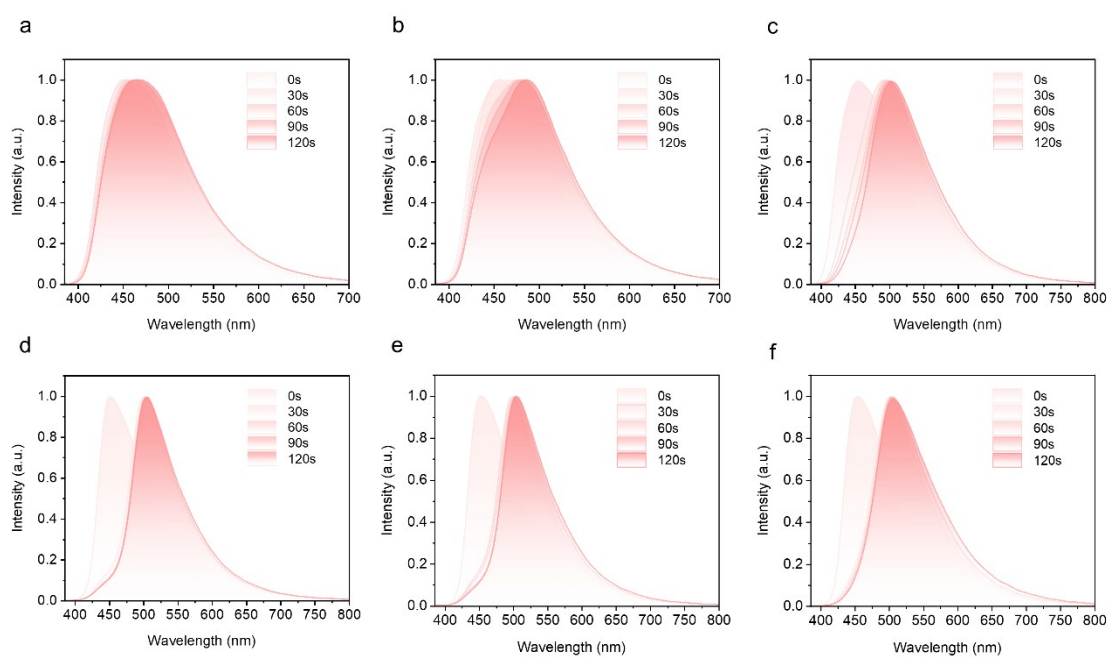


**Figure S16.** Time-dependent fluorescence spectra upon sunlight, 425 nm and 365 nm LEDs irradiation of Form I (a-c) and Form II (d-f).

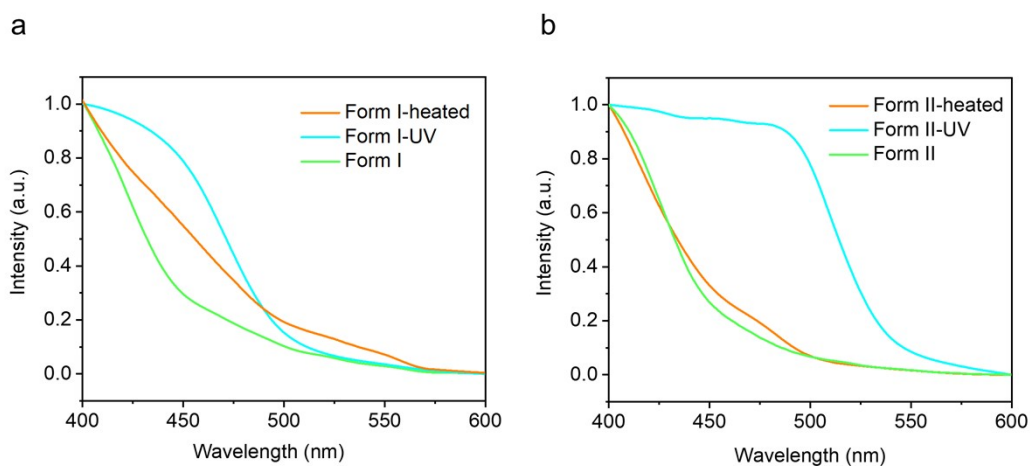


**Figure S17.** UV-vis absorption spectra of Form I (a) and Form II (b) upon UV irradiation and heating.

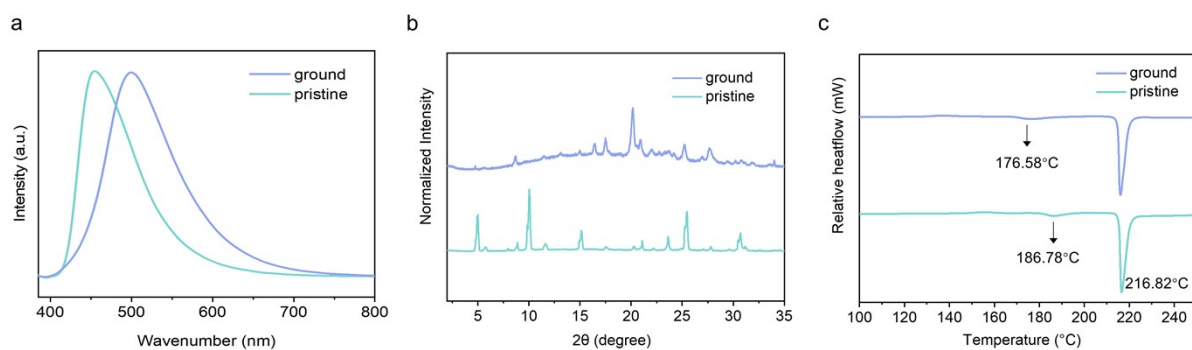


**Figure S18.** Fluorescence spectrum (a), PXRD (b) patterns and DSC (c) curves of pristine and ground samples of Form II.

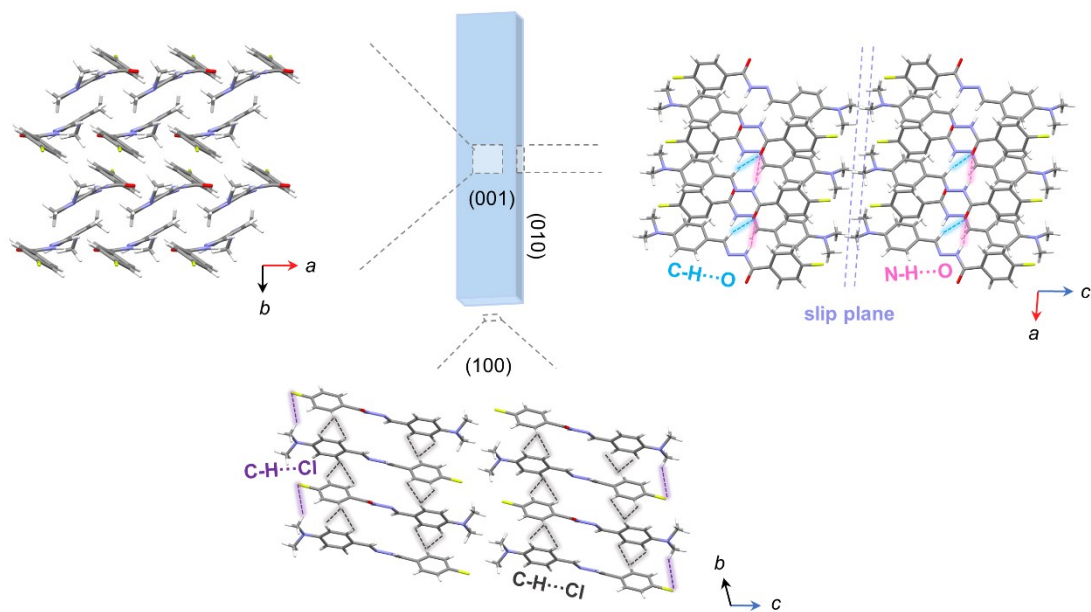


**Figure S19.** Molecular packing and intermolecular interactions of Form I.

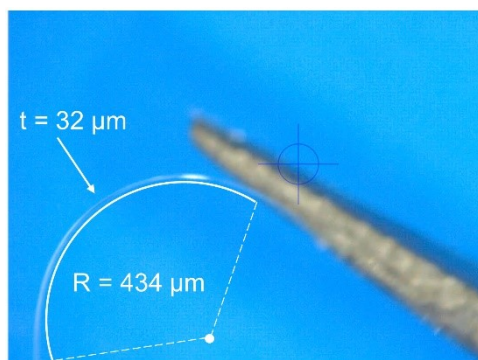


**Figure S20.** Elastic strain calculation of Form II crystals along the major crystal facet.

$$\varepsilon = \frac{t}{2R} = \frac{32}{2 \times 434} \times 100\% = 3.7\%$$

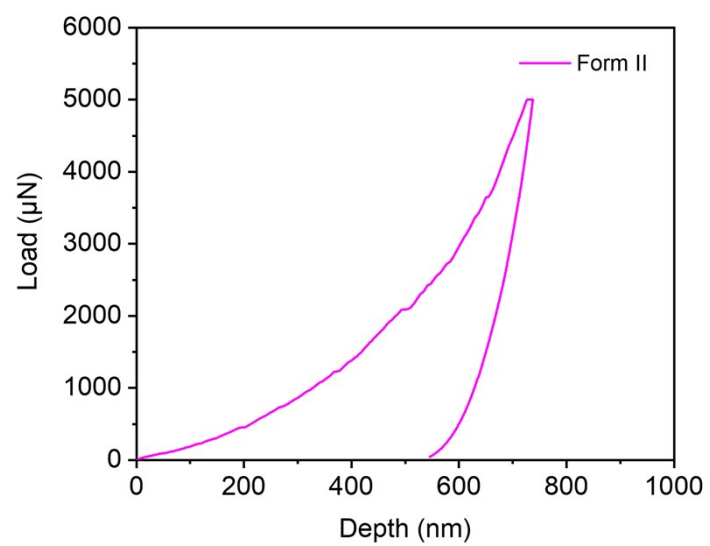
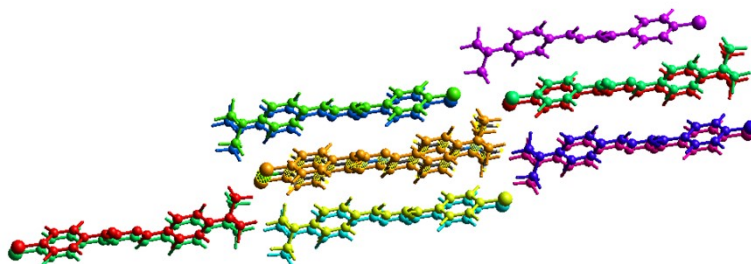


**Figure S21.** Load-depth (P-h) curves obtained by nanoindentation on the wide facets of crystals of Form II.

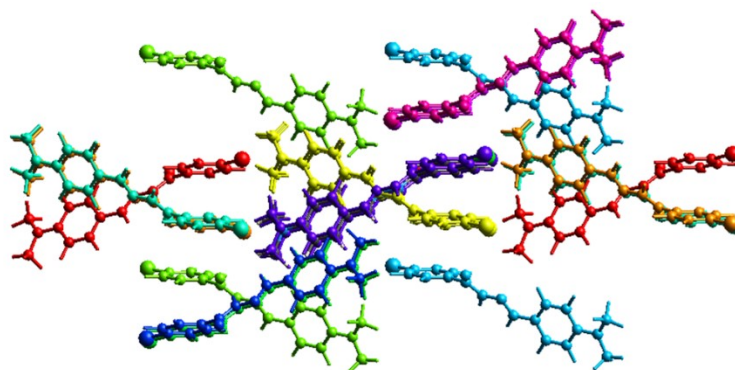


## Energy Frameworks

Crystal Explorer 17 was employed to calculate and visualize intermolecular interaction energies based on Gaussian B3LYP/6-31G (d, p) molecular wavefunctions. Atoms were generated within 3.8 Å. The tube size in the energy frameworks of both two polymorphs is 140, and the cut-off energy value is  $-20 \text{ kJ}\cdot\text{mol}^{-1}$ . The total energies of interaction between molecules include four components: electrostatic, polarization, dispersion and exchange-repulsion:  $E_{\text{tot}} = k_{\text{ele}}E_{\text{ele}} + k_{\text{pol}}E_{\text{pol}} + k_{\text{dis}}E_{\text{dis}} + k_{\text{rep}}E_{\text{rep}}$  where k refers to scale factor for benchmarked energy models.

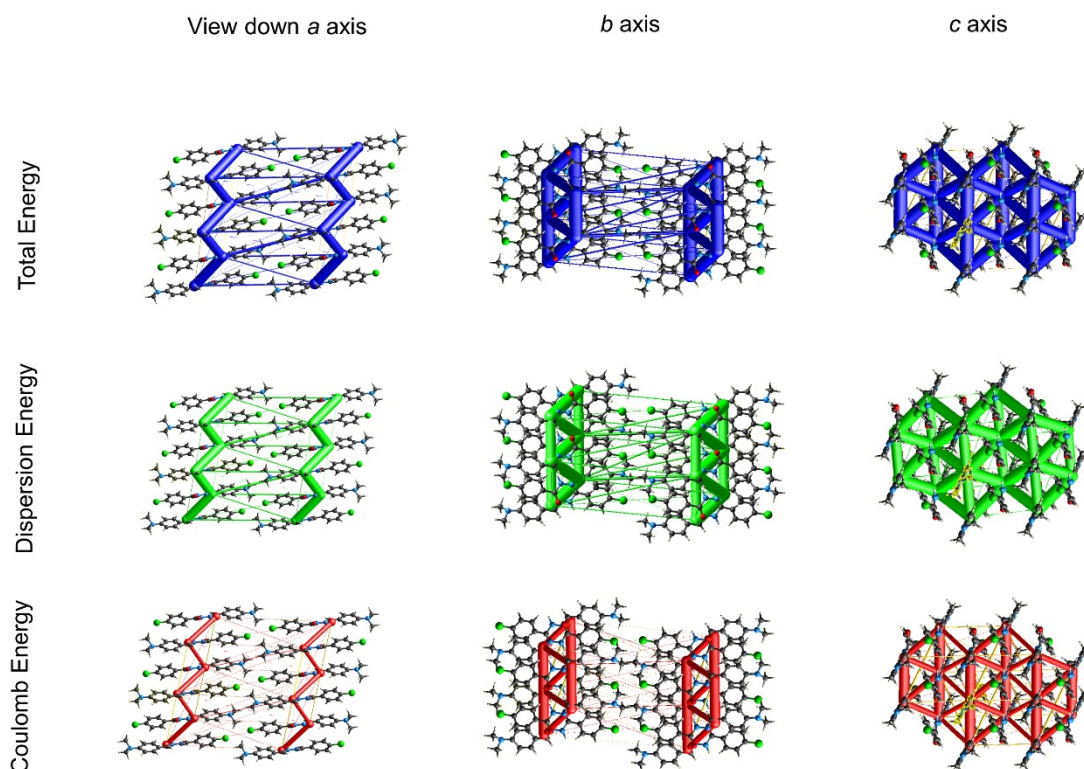


**Figure S22.** Interaction energies of Form I crystals.



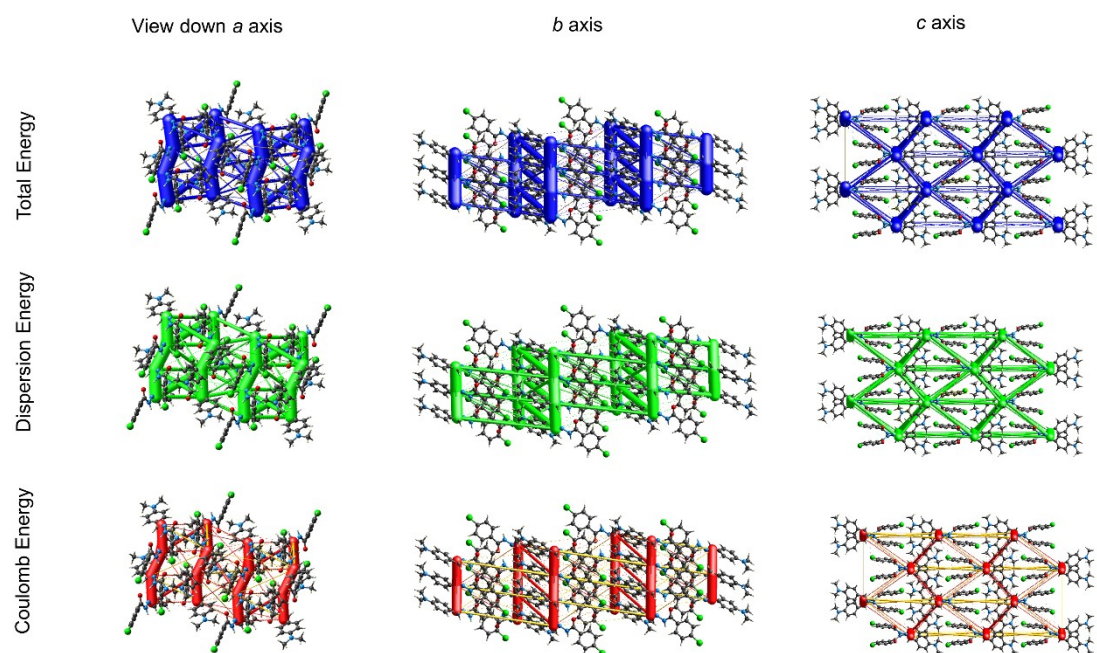
**Figure S23.** Interaction energies of Form II crystals.



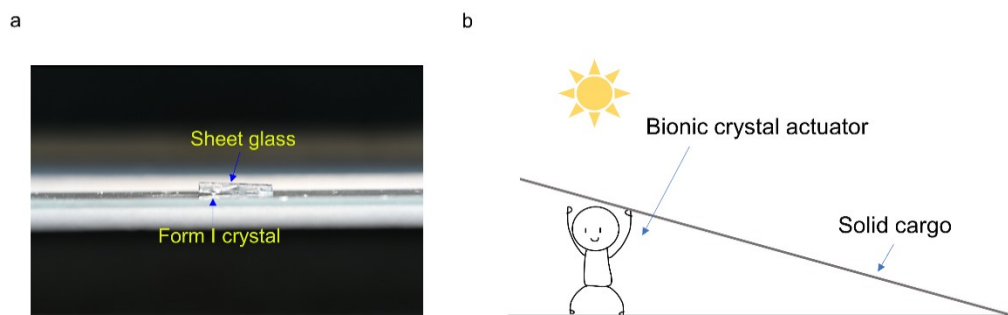


**Figure S24.** Energy frameworks corresponding to the electrostatic, dispersion and total interaction energy components of Form I.

As for Form I, along the growth axis, CDBB molecules stack via N-H $\cdots$ O ( $D, d, \theta = 3.067 \text{ \AA}, 2.242 \text{ \AA}, 156.02^\circ$ ) and C-H $\cdots$ O ( $3.242 \text{ \AA}, 2.448 \text{ \AA}, 141.03^\circ$ ) hydrogen bonds. Energy framework calculations reveal that the intermolecular interaction energy within the 1D stacked column is  $-118.2 \text{ kJ/mol}$ . The stacked column further extends along the *b*-axis through C-H $\cdots$  $\pi$  ( $3.611 \text{ \AA}, 2.770 \text{ \AA}, 148.02^\circ$ ) and ( $3.583 \text{ \AA}, 2.770 \text{ \AA}, 141.54^\circ$ ) hydrogen bonds ( $E_{\text{total}} = -194.1 \text{ kJ/mol}$ ), forming a two-dimension molecular layer. Simultaneously, viewing perpendicular to the (010) facet, it could be seen that there was a slip layer ( $E_{\text{total}} = -29.9 \text{ kJ/mol}$ ).



**Figure S25.** Energy frameworks corresponding to the electrostatic, dispersion and total interaction energy components of Form II.

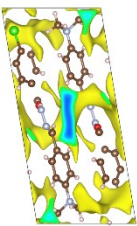
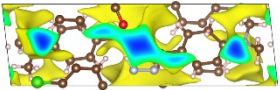
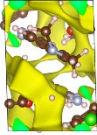
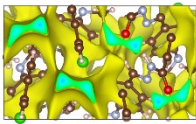
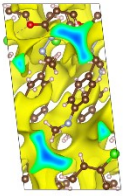
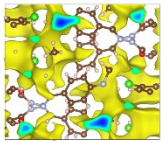


**Figure S26.** A picture and a schematic diagram of Form I holding up a glass sheet under natural light. The crystal can be regarded as a sun-driven bionic actuator to lift the cargo easily under sunlight.

**Table S1.** Crystallographic information of Form I, Form II crystal

Name	Form I	Form II
Formula	C <sub>16</sub> H <sub>16</sub> N <sub>3</sub> OCl	C <sub>16</sub> H <sub>16</sub> N <sub>3</sub> OCl
Crystal system	Triclinic	Monoclinic
Space group	<i>P</i> -1	<i>P</i> 2 <sub>1</sub> / <i>c</i>
a / Å	5.2898	14.9184
b / Å	7.8669	12.9302
c / Å	17.5590	7.6631
α / °	99.161	90
β / °	96.187	96.635
γ / °	90.692	90
Z, Z'	2,1	4,1
Cell volume / Å <sup>3</sup>	716.87	1468.3
R-factor (%)	3.59	6.43
CCDC number	2376850	2376851

**Table S2.** Fractional Free Volume of Form I and Form II.

Fractional Free Volume (FFV)	a-axis	b-axis	c-axis
28.06%	Form I		
			
	Form II		
29.81%			

**Table S3.** The interaction energies (kJ/mol) obtained from energy frameworks calculation for Form I. (scale factor are in table below)

	N	Sympo	R	Electron Density	E_ele	E_pol	E_dis	E_rep	E_tot
	2	x, y, z	17.78	B3LYP/6-31G(d,p)	-0.9	-0.4	-7.3	0.0	-7.5
	2	x, y, z	5.29	B3LYP/6-31G(d,p)	-41.4	-11.3	-48.8	57.5	-59.1
	1	-x, -y, -z	4.66	B3LYP/6-31G(d,p)	-17.3	-4.9	-53.1	33.6	-47.4
	1	-x, -y, -z	4.68	B3LYP/6-31G(d,p)	-25.3	-5.6	-61.3	47.5	-55.0
	2	x, y, z	17.56	B3LYP/6-31G(d,p)	0.1	-0.2	-4.7	0.0	-4.2
	1	-x, -y, -z	4.91	B3LYP/6-31G(d,p)	-17.8	-3.2	-59.9	44.8	-45.8
	1	-x, -y, -z	4.83	B3LYP/6-31G(d,p)	-23.4	-3.9	-56.1	49.6	-45.9
	1	-x, -y, -z	18.04	B3LYP/6-31G(d,p)	-2.4	-0.9	-13.4	0.0	-14.9
	1	-x, -y, -z	16.75	B3LYP/6-31G(d,p)	-0.6	-0.3	-6.5	0.0	-6.5
	1	-x, -y, -z	19.07	B3LYP/6-31G(d,p)	-0.1	-0.4	-7.4	0.0	-6.9

Energy Model	k_ele	k_pol	k_disp	k_rep
CE-HF ... HF/3-21G electron densities	1.019	0.651	0.901	0.811
CE-B3LYP ... B3LYP/6-31G(d,p) electron densities	1.057	0.740	0.871	0.618

**Table S4.** The interaction energies (kJ/mol) obtained from energy frameworks calculation for Form II. (scale factor are in table below)

	N	Symp	R	Electron Density	E_ele	E_pol	E_dis	E_rep	E_tot
	2	x, y, z	15.96	B3LYP/6-31G(d,p)	-2.1	-0.3	-5.7	0.0	-7.4
	2	x, -y+1/2, z+1/2	17.75	B3LYP/6-31G(d,p)	-3.3	-0.3	-5.4	0.0	-8.5
	2	x, -y+1/2, z+1/2	3.83	B3LYP/6-31G(d,p)	-51.0	-15.6	-70.8	86.3	-73.9
	2	-x, y+1/2, -z+1/2	10.52	B3LYP/6-31G(d,p)	-3.6	-2.0	-21.4	10.6	-17.4
	1	-x, -y, -z	11.85	B3LYP/6-31G(d,p)	-14.4	-3.2	-47.8	32.1	-39.4
	2	x, -y+1/2, z+1/2	14.97	B3LYP/6-31G(d,p)	10.4	-0.9	-16.6	0.0	-4.2
	2	-x, y+1/2, -z+1/2	10.18	B3LYP/6-31G(d,p)	-3.2	-0.6	-8.4	5.3	-7.8
	1	-x, -y, -z	10.57	B3LYP/6-31G(d,p)	0.0	-1.0	-19.5	12.8	-9.8
	2	x, y, z	7.66	B3LYP/6-31G(d,p)	-7.9	-2.2	-7.0	1.5	-15.2
	1	-x, -y, -z	9.30	B3LYP/6-31G(d,p)	4.7	-5.9	-27.3	12.9	-15.2
	1	-x, -y, -z	12.20	B3LYP/6-31G(d,p)	1.8	-0.8	-13.7	0.0	-10.5

Energy Model	k_ele	k_pol	k_disp	k_rep
CE-HF ... HF/3-21G electron densities	1.019	0.651	0.901	0.811
CE-B3LYP ... B3LYP/6-31G(d,p) electron densities	1.057	0.740	0.871	0.618

**Table S5.** Actuating performance indices of photosalient Form I crystals and photoinduced bending Form II crystals.

Performance Indices	Form I-push (365nm)				Form II-bend (365nm)			
	Range		Weighted mean	Weighted STD	Range		Weighted mean	Weighted STD
	min	max			min	max		
Normal Length (m)	$1.8 \times 10^{-3}$	$3.0 \times 10^{-3}$	$2.2 \times 10^{-3}$	$4.5 \times 10^{-4}$	$3.0 \times 10^{-3}$	$4.7 \times 10^{-3}$	$3.9 \times 10^{-3}$	$6.5 \times 10^{-4}$
Normal Width (m)	$2.8 \times 10^{-4}$	$5.5 \times 10^{-4}$	$4.3 \times 10^{-4}$	$8.8 \times 10^{-5}$	$6.5 \times 10^{-5}$	$1.4 \times 10^{-4}$	$1.0 \times 10^{-4}$	$2.9 \times 10^{-5}$
Normal Thickness (m)	$5.5 \times 10^{-5}$	$1.0 \times 10^{-4}$	$7.7 \times 10^{-5}$	$2.3 \times 10^{-5}$	$3.2 \times 10^{-5}$	$8.0 \times 10^{-5}$	$5.3 \times 10^{-5}$	$1.9 \times 10^{-5}$
Maximum Stroke (m)	$1.7 \times 10^{-5}$	$3.1 \times 10^{-5}$	$2.8 \times 10^{-5}$	$6.0 \times 10^{-6}$	$1.1 \times 10^{-4}$	$4.2 \times 10^{-4}$	$2.2 \times 10^{-4}$	$1.3 \times 10^{-4}$
Actuation Time (s)	7.0	11.0	9.0	1.4	4.0	17.0	10.0	5.1
Maximum Force Output (N)	$7.3 \times 10^{-4}$	$7.3 \times 10^{-4}$	$7.3 \times 10^{-4}$	0	$1.3 \times 10^{-6}$	$5.4 \times 10^{-6}$	$2.8 \times 10^{-6}$	$1.6 \times 10^{-6}$
Force Density ( $\text{N m}^{-3}$ )	$6.2 \times 10^6$	$1.6 \times 10^7$	$1.2 \times 10^7$	$3.8 \times 10^6$	$3.2 \times 10^4$	$4.1 \times 10^5$	$1.8 \times 10^5$	$1.3 \times 10^5$
Work Output (N m)	$1.3 \times 10^{-8}$	$2.7 \times 10^{-8}$	$2.1 \times 10^{-8}$	$4.5 \times 10^{-9}$	$5.2 \times 10^{-9}$	$2.4 \times 10^{-8}$	$1.2 \times 10^{-8}$	$8.2 \times 10^{-9}$
Work Density ( $\text{J m}^{-3}$ )	$1.6 \times 10^2$	$4.9 \times 10^2$	$3.3 \times 10^2$	$1.1 \times 10^2$	$1.3 \times 10^2$	$1.9 \times 10^3$	$7.3 \times 10^2$	$6.3 \times 10^2$
Power Output (kW)	$1.2 \times 10^{-12}$	$3.4 \times 10^{-12}$	$2.4 \times 10^{-12}$	$7.7 \times 10^{-13}$	$3.1 \times 10^{-13}$	$3.1 \times 10^{-12}$	$1.4 \times 10^{-12}$	$9.7 \times 10^{-13}$
Power Density ( $\text{W m}^{-3}$ )	$1.9 \times 10^1$	$3.1 \times 10^2$	$9.1 \times 10^1$	$1.1 \times 10^2$	7.4	$3.2 \times 10^2$	$1.0 \times 10^2$	$1.1 \times 10^2$



**Table S6.** Actuating performance indices for photoinduced bending of Form I crystals upon 365nm LED and sunlight irradiation.

Performance Indices	Form I-lift (365nm)				Form I-lift (sun)			
	Range		Weighted mean	Weighted STD	Range		Weighted mean	Weighted STD
	min	max			min	max		
Normal Length (m)	$5.0 \times 10^{-3}$	$6.1 \times 10^{-3}$	$5.4 \times 10^{-3}$	$4.2 \times 10^{-4}$	$6.3 \times 10^{-3}$	$7.9 \times 10^{-3}$	$7.1 \times 10^{-3}$	$6.7 \times 10^{-4}$
Normal Width (m)	$6.8 \times 10^{-5}$	$8.1 \times 10^{-5}$	$7.4 \times 10^{-5}$	$4.6 \times 10^{-6}$	$6.1 \times 10^{-5}$	$7.5 \times 10^{-5}$	$6.9 \times 10^{-5}$	$5.8 \times 10^{-6}$
Normal Thickness (m)	$4.2 \times 10^{-5}$	$5.2 \times 10^{-5}$	$4.8 \times 10^{-5}$	$3.6 \times 10^{-6}$	$4.7 \times 10^{-5}$	$5.8 \times 10^{-5}$	$5.3 \times 10^{-5}$	$4.9 \times 10^{-6}$
Maximum Stroke (m)	$9.0 \times 10^{-5}$	$1.5 \times 10^{-4}$	$1.2 \times 10^{-4}$	$2.3 \times 10^{-5}$	$9.0 \times 10^{-5}$	$1.5 \times 10^{-4}$	$1.2 \times 10^{-4}$	$2.3 \times 10^{-5}$
Actuation Time (s)	4.0	6.0	5.3	$8.3 \times 10^{-1}$	580	622	608	$1.2 \times 10^1$
Maximum Force Output (N)	$8.0 \times 10^{-3}$	$1.2 \times 10^{-2}$	$9.7 \times 10^{-3}$	$1.4 \times 10^{-3}$	$1.6 \times 10^{-3}$	$2.1 \times 10^{-3}$	$1.9 \times 10^{-3}$	$2.5 \times 10^{-4}$
Force Density ( $\text{N m}^{-3}$ )	$4.4 \times 10^8$	$5.6 \times 10^8$	$5.0 \times 10^8$	$5.5 \times 10^7$	$6.9 \times 10^7$	$8.4 \times 10^7$	$7.4 \times 10^7$	$6.9 \times 10^6$
Work Output (N m)	$8.3 \times 10^{-7}$	$1.5 \times 10^{-6}$	$1.1 \times 10^{-6}$	$2.3 \times 10^{-7}$	$6.2 \times 10^{-7}$	$1.3 \times 10^{-6}$	$9.7 \times 10^{-7}$	$2.6 \times 10^{-7}$
Work Density ( $\text{J m}^{-3}$ )	$4.2 \times 10^4$	$8.4 \times 10^4$	$6.0 \times 10^4$	$1.5 \times 10^4$	$2.8 \times 10^4$	$5.0 \times 10^4$	$3.8 \times 10^4$	$9.4 \times 10^3$
Power Output (kW)	$1.7 \times 10^{-10}$	$2.9 \times 10^{-10}$	$2.2 \times 10^{-10}$	$4.3 \times 10^{-11}$	$1.0 \times 10^{-12}$	$2.1 \times 10^{-12}$	$1.6 \times 10^{-12}$	$4.3 \times 10^{-13}$
Power Density ( $\text{W m}^{-3}$ )	$9.5 \times 10^3$	$1.7 \times 10^4$	$1.2 \times 10^4$	$3.0 \times 10^3$	$4.6 \times 10^1$	$8.3 \times 10^1$	$6.2 \times 10^1$	$1.6 \times 10^1$